Inorganica Chimica Acta 373 (2011) 201–210

Contents lists available at ScienceDirect

Inorganica Chimica Acta

journal homepage: www.elsevier.com/locate/ica

Structure and properties of cobalt *ortho*-phenylenediacetate coordination polymers with rigid dipyridyl ligands

Karyn M. Blake, Arash Banisafar, Robert L. LaDuca *

Lyman Briggs College and Department of Chemistry, Michigan State University, East Lansing, MI 48825, USA

ARTICLE INFO

Article history:
Received 25 January 2011
Accepted 15 April 2011
Available online 23 April 2011

Keywords:
Cobalt
Coordination polymer
Thermal analysis
Anion dependence
Topology
Ferromagnetism

ABSTRACT

Divalent cobalt coordination polymers containing both *ortho*-phenylenediacetate (ophda) and rigid dipyridyl ligands 4,4′-bipyridine (bpy) or 1,2-bis(4-pyridyl)ethylene (dpee) display different topologies depending on carboxylate binding mode, tether length, and inclusion of charged species. $[Co(ophda)(H_2O)(dpee)]_n$ (**1**) displays a common (4,4) grid layer motif. Use of the shorter bpy tether afforded $\{[Co_2(ophda)_2(bpy)_3(H_2O)_2][Co(bpy)_2(H_2O)_4](NO_3)_2\cdot 2bpy\cdot 7H_2O\}_n$ (**2**) or $[Co(ophda)(bpy)]_n$ (**3**) depending on cobalt precursor. Compound **2** manifests 5-connected $[Co_2(ophda)_2(bpy)_3(H_2O)_2]_n$ pillared bilayer slabs with rare 4^86^2 SnS topology and entrained $[Co(bpy)_2(H_2O)_4]^{2+}$ complex cations. The 3-D coordination polymer **3** has an uncommon 4,6-connected binodal $(4^46^2)(4^46^{10}8)$ **fsc** topology, and shows ferromagnetic coupling ($J = +1.5(2)\ cm^{-1}$) along 1-D *spiro*-fused $[Co(OCO)_2]_n$ chain submotifs.

1. Introduction

Divalent metal coordination polymers constructed from aromatic dicarboxylate ligands show potential industrial applications [1], including gas storage [2], selective separation [3], ion exchange [4], catalysis [5], luminescence [6], and non-linear optical second harmonic generation [7]. Different coordination geometries and a multitude of possible carboxylate binding modes can promote a wide range of structural topologies [8]. Cobalt dicarboxylate coordination polymers often manifest magnetic properties [9] such as spin canting [10], metamagnetism [11], and single-chain magnetism [12]. Structural elaboration and topological variance in these materials can be enhanced by the incorporation of neutral ligands such as 4,4′-bipyridine (bpy), 1,2-bis(4-pyridyl)ethane (dpe), or 1,2-bis(4-pyridyl)ethylene (dpee) via adjustment of the carboxylate bridging mode [13–15].

A large number of previously reported divalent cobalt coordination polymers have been constructed from isomeric benzenedicarboxylate ligands such as phthalate (pht) [16], isophthalate (iph) [17], terephthalate [18], which provide both the charge balance and structural rigidity necessary for self-assembly. In these phases, the geometric disposition of the rigid but twistable carboxylate arms and the nature of the neutral tethering ligand play a predominant role in enforcing the final topology. For example, $[Co(Hpht)_2(bpy)]_n$ possesses a 6-connected self-penetrated 3-D network built from a diamondoid $[Co(Hpht)_2]_n$ subnet with crossing bpy tethers [13], while $[Co(pht)(dpe)(H_2O)]_n$ exhibits a standard (4,4) grid layer topology with *anti-syn* bridged dinuclear $\{Co_2(O-CO)_2\}$ units and exotridentate pht ligands [14]. $[Co(iph)(dpee)]_n$ has a similar dimer-based (4,4) grid underlying topology as $[Co(pht)(dpe)(H_2O)]_n$ [15], despite the wider separation of carboxylate arms within the benzenedicarboxylate component.

In comparison to benzenedicarboxylates, phenylenediacetate ligands (phda) have seen more infrequent use to date in this chemistry [19–24]. The increased conformational flexibility of the pendant acetate arms of the isomeric phda ligands can result in variable carboxylate binding modes, providing access to various coordination polymer topologies. Utilizing the long-spanning bis(4-pyridylmethyl)piperazine (4-bpmp) as a neutral co-ligand, a series of cobalt phda coordination polymers were recently prepared in our laboratory [24]. $\{[Co(pphda)(4\text{-}bpmp)(H_2O)_2]\cdot 2H_2O\}_n$ (pphda = *para*-phenylenediacetate) has a standard (4,4) rhomboid grid topology, while $[Co(mphda)(4\text{-}bpmp)]_n$ (mphda = *meta*-phenylenediacetate) possesses dinuclear $\{Co_2(OCO)_2\}$ units linked into a 6-connected primitive cubic topology. The ophda (*ortho*-phenylenediacetate) congener $\{[Co(ophda)(4\text{-}bpmp)_{1.5}(H_2O)](H_2O\text{-}bpmp)_{0.5}(ClO_4)\cdot 12H_2O\}_n$ is a very rare example of a 5-connected layered net, with a unique Archimedean topology consisting of triangular and rectangular circuits.

A search of the Cambridge Structural Database [25] revealed a great paucity of cobalt phenylenediacetate coordination polymers, so we attempted to prepare cobalt ophda phases incorporating the shorter, more rigid dipyridyl linkers bpy and dpee (Scheme 1). Herein we report the synthesis, crystal structures, and thermal degradation properties of three cobalt ophda coordination polymers with diverse 2-D and 3-D topologies: $[Co(ophda)(dpee)(H_2O)]_n$ (**1**),

* Corresponding author. Address: Lyman Briggs College, E-30 Holmes Hall, Michigan State University, East Lansing, MI 48825, USA. Tel.: +1 517 432 2268.
E-mail addresses: laduca@msu.edu, laduca@chemistry.msu.edu (R.L. LaDuca).

0020-1693/$ - see front matter © 2011 Elsevier B.V. All rights reserved.
doi:10.1016/j.ica.2011.04.029

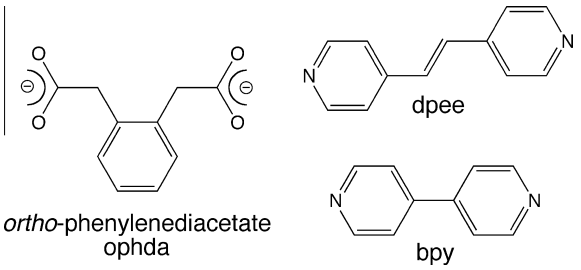

Scheme 1. Ligands used in this study.

$\{[Co_2(ophda)_2(bpy)_3(H_2O)_2][Co(bpy)_2(H_2O)_4](NO_3)_2{\cdot}2bpy{\cdot}7H_2O\}_n$ (**2**), and $[Co(ophda)(bpy)]_n$ (**3**). The variable temperature magnetic susceptibility behavior of **3** was also probed, as it contains paramagnetic d^7 ions in proximity, bridged by carboxylate groups.

2. Experimental

2.1. General considerations

All chemicals were commercially obtained from Aldrich. Water was deionized above 3 MΩ cm in-house. Thermogravimetric analysis was performed on a TA Instruments TGA 2050 Thermogravimetric Analyzer with a heating rate of 10 °C/min up to 900 °C. Elemental Analysis was carried out using a Perkin–Elmer 2400 Series II CHNS/O Analyzer. IR spectra were recorded on powdered samples using a Perkin–Elmer Spectrum One instrument. Variable temperature magnetic susceptibility data (2 K to 300 K) for **3** were collected on a Quantum Design MPMS SQUID magnetometer at an applied field of 0.1 T. After each temperature change the sample was kept at the new temperature for 5 min before magnetization measurement to ensure thermal equilibrium. The susceptibility data was corrected for diamagnetism using Pascal's constants [26].

2.2. Preparation of $[Co(ophda)(dpee)(H_2O)]_n$ (*1*)

$Co(NO_3)_2{\cdot}6H_2O$ (28 mg, 0.096 mmol), *ortho*-phenylenediacetic acid (19 mg, 0.096 mmol) and 1,2-di(4-pyridyl)ethylene (17 mg, 0.096 mmol) were placed into 10 mL distilled H_2O in a 23 mL Teflon-lined Parr acid digestion bomb. The bomb was sealed and heated at 120 °C for 48 h, whereupon it was cooled slowly to 25 °C. Pink blocks of **1** (33 mg, 76% yield based on Co) were isolated after washing with distilled water and acetone, and drying in air. *Anal.* Calc. for $C_{22}H_{20}CoN_2O_5$ **1**: C, 58.55; H, 4.47; N, 6.21. Found: C, 58.12; H, 4.09; N, 5.94%. IR (cm^{-1}): 3200 (w, br), 3035 (w), 1607 (w), 1556 (s), 1400 (s), 1283 (w), 1215 (w), 1215 (w), 1153 (w), 1016 (m), 972 (w), 938 (w), 830 (s), 723 (s).

2.3. Preparation of $\{[Co_2(ophda)_2(bpy)_3(H_2O)_2][Co(bpy)_2(H_2O)_4](NO_3)_2{\cdot}2bpy{\cdot}7H_2O\}_n$ (*2*)

$Co(NO_3)_2{\cdot}6H_2O$ (28 mg, 0.096 mmol), *ortho*-phenylenediacetic acid (19 mg, 0.096 mmol) and 4,4′-bipyridine (28 mg, 0.18 mmol) were placed into 10 mL distilled H_2O in a 23 mL Teflon-lined Parr acid digestion bomb. The bomb was sealed and heated at 120 °C for 48 h, whereupon it was cooled slowly to 25 °C. Pink blocks of **2** (33 mg, 0.016 mmol, 64% yield based on the limiting reactant bpy) were isolated after washing with distilled water and acetone, and drying in air. *Anal.* Calc. for $C_{90}H_{88}Co_3N_{16}O_{27}$ **2**: C, 53.98; H, 4.43; N, 11.19. Found: C, 53.23; H, 4.13; N, 10.97%. IR (cm^{-1}): 3259 (w, br), 2821 (w), 1586 (s), 1566 (s), 1532 (s), 1486 (m), 1411 (m), 1378 (s), 1322 (m), 1255 (w), 1219 (m), 1159 (w), 1120 (w), 1065 (m), 1045 (w), 1007 (w), 812 (s), 807 (s), 730 (s), 673 (w).

2.4. Preparation of $[Co(ophda)(bpy)]_n$ (*3*)

$Co(CH_3COO)_2{\cdot}4H_2O$ (111 mg, 0.44 mmol), *ortho*-phenylenediacetic acid (86 mg, 0.44 mmol), and 4,4′-bipyridine (87 mg, 0.56 mmol), were placed into 8 mL distilled H_2O in a Teflon-lined 23 mL Parr acid digestion bomb. The bomb was sealed and heated at 150 °C for 36 h, whereupon it was cooled slowly in air to 25 °C. Orange crystals of **3** (69 mg, 38% yield based on Co) were isolated after washing with distilled water and acetone and drying in air. *Anal.* Calc. for $C_{20}H_{16}CoN_2O_4$: C, 58.98; H, 3.96; N, 6.88. Found: C, 58.54; H, 3.67; N, 6.64%. IR (cm^{-1}): 2950 (w), 1628 (w), 1603 (w), 1566 (s), 1486 (w), 1438 (w), 1413 (w), 1373 (s), 1317 (w), 1219 (w), 1072 (w), 1047 (w), 924 (w), 853 (w), 825 (s), 745 (w), 716 (s), 670 (w).

2.5. X-ray crystallography

Single crystal X-ray diffraction data for **1**–**3** were collected with a Bruker-AXS SMART 1k CCD instrument at 173 K. Reflection data were acquired using graphite-monochromated Mo Kα radiation (λ = 0.71073 Å). The data was integrated via SAINT [27]. Lorentz and polarization effect and empirical absorption corrections were applied with SADABS [28]. The structures were solved using direct methods and refined on F^2 using SHELXTL [29]. All non-hydrogen atoms were refined anisotropically. Hydrogen atoms bound to carbon atoms were placed in calculated positions and refined

Table 1
Crystal and structure refinement data for **1**–**3**.

Data	1	2	3
Empirical Formula	$C_{22}H_{20}CoN_2O_5$	$C_{90}H_{88}Co_3N_{16}O_{27}$	$C_{20}H_{16}CoN_2O_4$
Formula weight	451.33	2002.55	407.28
Crystal system	monoclinic	triclinic	monoclinic
Space group	$P2_1/c$	$P\bar{1}$	$P2/c$
a (Å)	12.1087(19)	9.7248(14)	9.0714(11)
b (Å)	19.386(3)	11.4547(16)	11.4336(14)
c (Å)	8.5589(140	21.894(3)	9.6453(12)
α (°)	90	94.697(2)	90
β (°)	98.890(5)	92.004(2)	116.633(1)
γ (°)	90	108.930(2)	90
V (Å^3)	1985.0(5)	2294.4(6)	894.25(2)
Z	4	1	2
D_{calc} (g cm^{-3})	1.510	1.449	1.513
μ (mm^{-1})	0.902	0.624	0.988
Minimum/maximum transmission	0.7882/0.9412	0.8657/0.9448	0.6472/0.8530
hkl Ranges	$-15 \le h \le 15$, $-25 \le k \le 25$, $-11 \le l \le 10$	$-11 \le h \le 11$, $-13 \le k \le 13$, $-26 \le l \le 26$	$-11 \le h \le 11$, $-13 \le k \le 14$, $-12 \le l \le 12$
Unique reflections	4 498	8 439	2 020
R(int)	0.1000	0.0134	0.0220
Parameters/restraints	277/3	634/12	125/0
R_1 (all data)	0.0719	0.1034	0.0315
R_1 ($I > 2\sigma(I)$)	0.0490	0.0761	0.0287
wR_2 (all data)	0.0905	0.1867	0.0811
wR_2 ($I > 2\sigma(I)$)	0.0842	0.1734	0.0788
Max/min residual (e$^-$ Å^3)	0.550/–0.654	0.944/–0.578	0.979/0.992
Goodness-of-fit (GOF)	0.942	1.078	1.144

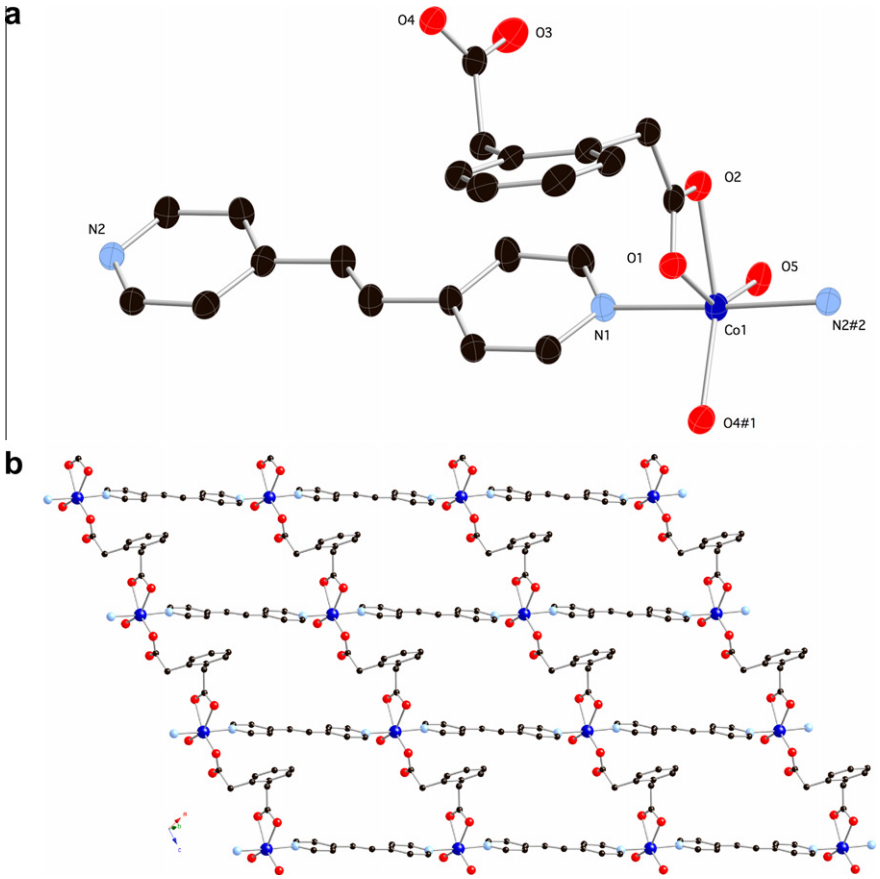

Fig. 1. (a) Coordination environment in **1**. Symmetry codes refer to those in Table 2. (b) A single $[Co(ophda)(dpee)(H_2O)]_n$ layer in **1**.

isotropically with a riding model. Relevant crystallographic data for **1**–**3** is listed in Table 1.

3. Results and discussion

3.1. Synthesis and spectral characterization

Compounds **1**–**3** were prepared under hydrothermal conditions *via* reaction of a cobalt salt, *ortho*-phenylenediacetic acid, and the appropriate dipyridine. The infrared spectra of all compounds corresponded with their single crystal structures. Medium intensity bands in the range of ~1600 cm^{-1} to ~1200 cm^{-1} can be ascribed to stretching modes of the pyridyl rings of the nitrogen base ligands and the aromatic rings of the ophda ligands [30]. Puckering modes of the pyridyl and/or phenyl rings are evident in the region between 820 cm^{-1} and 600 cm^{-1}. Asymmetric and symmetric C–O stretching modes of the fully deprotonated phda ligands correspond to the strong, broadened features at 1551 cm^{-1} and 1400 cm^{-1} (for **1**), 1532 cm^{-1} and 1378 cm^{-1} (for **2**), and 1566 cm^{-1} and 1373 cm^{-1} (for **3**). The absence of any bands in the region of 1700 cm^{-1} signifies full deprotonation of the acid precursor. Broadened yet weak bands in the region of ~3200 cm^{-1} to ~3400 cm^{-1} in **1** and **2** represent O–H stretching modes within the aqua ligands or co-crystallized water molecules. The band at 3035 cm^{-1} in the spectrum of **1** is indicative of the alkenyl C–H bonds. The broadness of these higher energy spectral features is caused by the hydrogen bonding present in all cases (see below).

Table 2
Selected bond distance (Å) and angle (°) data for **1**.

Co1–O5	2.0465(19)	N1–Co1–$N2^{\#2}$	177.49(8)
Co1–$O4^{\#1}$	2.0930(18)	O5–Co1–O2	88.46(8)
Co1–N1	2.144(2)	$O4^{\#1}$–Co1–O2	147.78(7)
Co1–$N2^{\#2}$	2.145(2)	N1–Co1–O2	86.20(7)
Co1–O2	2.1884(18)	$N2^{\#2}$–Co1–O2	91.29(8)
Co1–O1	2.2608(18)	O5–Co1–O1	147.26(8)
O5–Co1–$O4^{\#1}$	123.53(8)	$O4^{\#1}$–Co1–O1	89.20(7)
O5–Co1–N1	89.55(8)	N1–Co1–O1	91.53(7)
$O4^{\#1}$–Co1–N1	90.00(8)	$N2^{\#2}$–Co1–O1	87.01(7)
O5–Co1–$N2^{\#2}$	90.58(8)	O2–Co1–O1	58.99(6)
$O4^{\#1}$–Co1–$N2^{\#2}$	92.01(8)		

Symmetry transformations to generate equivalent atoms: #1 *x*, *y*, *z* + 1; #2 *x* + 1, *y*, *z* + 1.

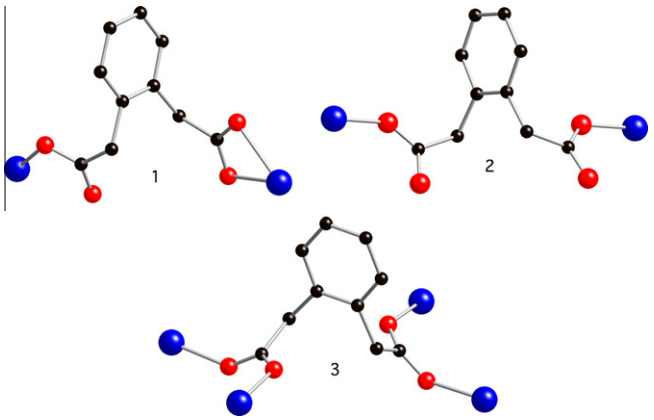

Scheme 2. Binding modes of ophda ligands in **1**–**3**.

Table 3
Hydrogen bonding distance (Å) and angle (°) data for **1** and **2**.

D–H···*A*	d(H···*A*)	∠DHA	d(*D*···*A*)	Symmetry transformation for *A*
1				
O5–H5A···O2	1.929(16)	2.743(2)	172(3)	$x, -y+3/2, z+1/2$
O5–H5B···O3	1.787(15)	2.646(3)	177(3)	$x, -y+3/2, z+1/2$
2				
O1W–H1WB···N6	2.05(3)	2.932(9)	172(6)	
O1W–H1WA···O12	2.23	3.084(17)	179.5	
O2W–H2WA···O11	2.13	2.977(18)	179.0	$x, y-1, z$
O2W–H2WB···O3W	2.38(11)	3.121(18)	141(14)	$-x-1, -y, -z+1$
O6–H6A···O2W	1.79(2)	2.671(8)	177(6)	$-x, -y, -z+1$
O6–H6B···O8	1.86(2)	2.739(7)	170(6)	
O5–H5B···O2	1.80(3)	2.633(6)	158(6)	$-x, -y+1, -z+1$
O5–H5A···N8	1.86(2)	2.738(6)	175(6)	$-x-1, -y, -z+1$

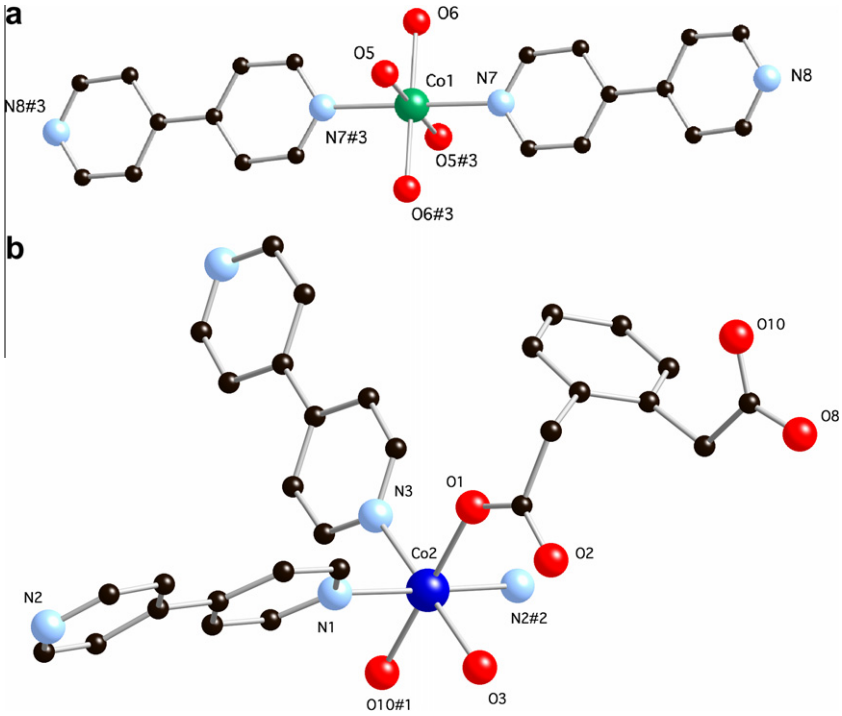

Fig. 2. (a) $[Co(H_2O)_4(bpy)_2]^{2+}$ coordination complex cation in **2**. (b) Coordination environment at Co2 in **2**. Symmetry codes refer to those in Table 4.

Table 4
Selected bond distance (Å) and angle (°) data for **2**.

Co1–O5	2.033(4)	$O10^{\#1}$–Co2–O1	179.34(15)
Co1–O6	2.117(5)	$O10^{\#1}$–Co2–O3	89.30(15)
Co1–N7	2.194(5)	O1–Co2–O3	90.86(15)
Co2–$O10^{\#1}$	2.049(3)	$O10^{\#1}$–Co2–N3	88.52(15)
Co2–O1	2.079(3)	O1–Co2–N3	91.34(15)
Co2–O3	2.120(4)	O3–Co2–N3	177.22(17)
Co2–N3	2.148(4)	$O10^{\#1}$–Co2–N1	88.51(15)
Co2–N1	2.168(4)	O1–Co2–N1	90.85(14)
Co2–$N2^{\#2}$	2.195(4)	O3–Co2–N1	89.68(17)
O5–Co1–$O5^{\#3}$	180	N3–Co2–N1	91.99(16)
O5–Co1–O6	92.06(19)	$O10^{\#1}$–Co2–$N2^{\#2}$	90.31(15)
$O5^{\#3}$–Co1–O6	87.94(19)	O1–Co2–$N2^{\#2}$	90.32(14)
O6–Co1–$O6^{\#3}$	180	O3–Co2–$N2^{\#2}$	93.05(17)
O5–Co1–N7	89.58(17)	N3–Co2–$N2^{\#2}$	85.24(16)
$O5^{\#3}$–Co1–N7	90.42(17)	N1–Co2–$N2^{\#2}$	177.01(16)
O6–Co1–N7	93.4(2)		
$O6^{\#3}$–Co1–N7	86.6(2)		
$N7^{\#3}$–Co1–N7	180		

Symmetry transformations to generate equivalent atoms: #1 $x-1, y, z$; #2 $x, y-1, z$; #3 $-x, -y+1, -z+1$.

The band at 1219 cm^{-1} in the spectrum of **2** is assigned to N–O stretching modes of the unligated nitrate ions.

3.2. Structural description of $[Co(ophda)(dpee)(H_2O)]_n$ (**1**)

The asymmetric unit of compound **1** comprises a divalent cobalt atom, an ophda ligand, a dpee ligand, and one ligated water molecule. The coordination environment at cobalt is a distorted $\{CoN_2O_4\}$ octahedron with trans dpee pyridyl donor ligands in the axial positions, with the equatorial plane containing one monodentate ophda carboxylate group, one chelating ophda carboxylate group, and an aqua ligand (Fig. 1a). Relevant bond lengths and angles within the coordination environment are listed in Table 2.

$[Co(ophda)(H_2O)]_n$ chains are oriented parallel to the *c* crystal direction in **1**, formed by junction of cobalt atoms through ophda tethering ligands with a μ_2-κ^3-O,O′:O″ chelating/monodentate binding mode (Scheme 2). The 129.9° torsion angle between the pendant acetate arms of the ophda ligands provides a Co···Co distance of 8.559 Å. Parallel $[Co(ophda)(H_2O)]_n$ chains are pillared into a standard (4,4) rhomboid grid $[Co(ophda)(H_2O)(dpee)]_n$ motif

Table 5
Selected bond distance (Å) and angle (°) data for **3**.

Co1–O2	2.0302(12)
Co1–O1$^{\#1}$	2.1585(12)
Co1–N1	2.166(2)
Co1–N2$^{\#2}$	2.180(2)
O2$^{\#3}$–Co1–O2	174.60(7)
O2–Co1–O1$^{\#1}$	90.70(5)
O2–Co1–O1$^{\#4}$	88.86(5)
O1$^{\#1}$–Co1–O1$^{\#4}$	170.59(6)
O2–Co1–N1	87.30(3)
O1$^{\#1}$–Co1–N1	85.29(3)
O2–Co1–N2$^{\#2}$	92.70(3)
O1$^{\#1}$–Co1–N2$^{\#2}$	94.71(3)
N1–Co1–N2$^{\#2}$	180.0

Symmetry transformation to generate equivalent atoms: #1 $-x+2, -y, -z$; #2 $x, y-1, z$; #3 $-x+2, y, -z-1/2$; #4 $x, -y, z+1/2$.

(Fig. 1b) by rigid dpee tethers, which span a Co···Co distance of 13.706 Å. The through-space Co···Co distances across the pinched grid apertures measure 12.109 × 19.380 Å, with Co···Co···Co angles around the grid perimeters subtending 60.8 and 119.2°. [Co(ophda)(H_2O)(dpee)]$_n$ layers stack in an offset *ABAB* pattern along the *b* crystal direction (Fig. S1), with hydrogen bonding between the aqua ligands and oxygen atoms within chelating ophda carboxylate groups or unligated oxygen atoms within the monodentate ophda termini providing the necessary supramolecular interactions (Table 3).

3.3. Structural description of $\{[Co_2(ophda)_2(bpy)_3(H_2O)_2][Co(bpy)_2(H_2O)_4](NO_3)_2{\cdot}2bpy{\cdot}7H_2O\}_n$ (**2**)

The large asymmetric unit of compound **2** contains a cobalt atom (Co1) on a crystallographic inversion center and another cobalt atom (Co2) on a general position, two and one-half bpy molecules bound to cobalt, three aqua ligands, one unligated bpy molecule, and one nitrate counterion, along with three and one-half water molecules of crystallization. The coordination environment at Co1 is a distorted {CoN_2O_4} octahedron with four aqua ligands in the equatorial plane and trans nitrogen donors from two pendant, monodentate bpy ligands to construct isolated $[Co(H_2O)_4(bpy)_2]^{2+}$ coordination complexes (Fig. 2a). The coordination environment at Co2 is a distorted {CoN_3O_3} octahedron, with

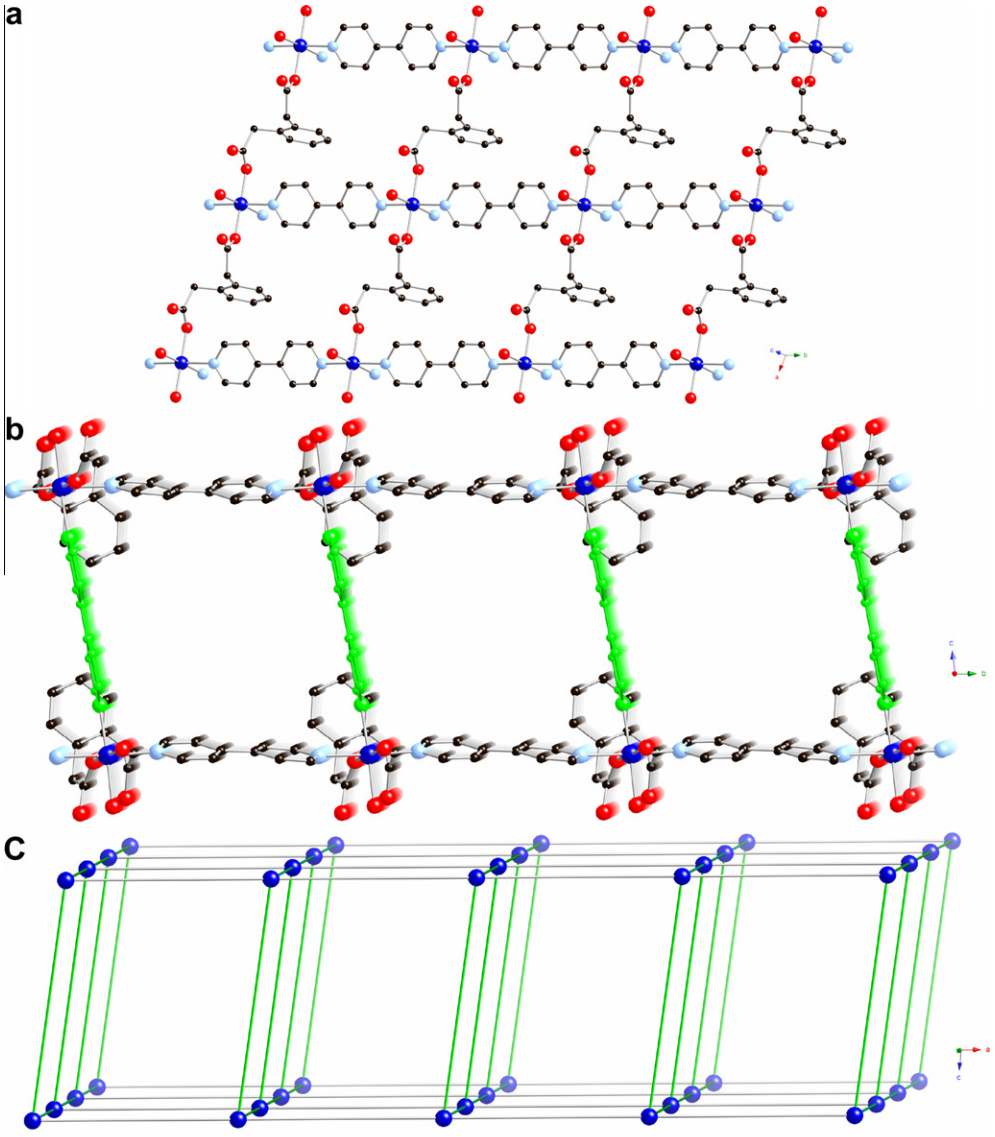

Fig. 3. Structural submotifs in **2**. (a) [Co(ophda)(bpy)(H_2O)]$_n$ layer (b) neutral [Co_2(ophda)$_2$(bpy)$_3$(H_2O)$_2$]$_n$ slab (c) Network representation of the 5-connected $4^8 6^2$ SnS topology slab.

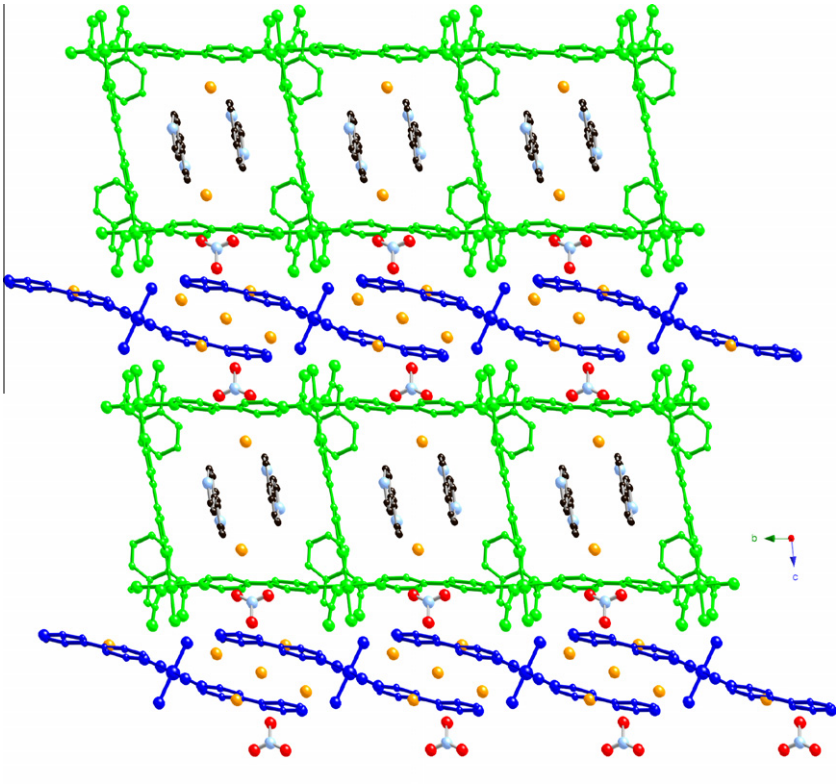

Fig. 4. Supramolecular structure of **2**. In the online version of this article, the neutral $[Co_2(ophda)_2(bpy)_3(H_2O)_2]_n$ slabs appear green, the $[Co(H_2O)_4(bpy)_2]^{2+}$ coordination complex cations appear blue, and the unligated water molecules appear orange. Unligated bpy molecules are positioned within apertures in the slab units, while nitrate counteranions rest in the inter-slab regions. (For interpretation of the references to colour in this figure legend, the reader is referred to the web version of this article.)

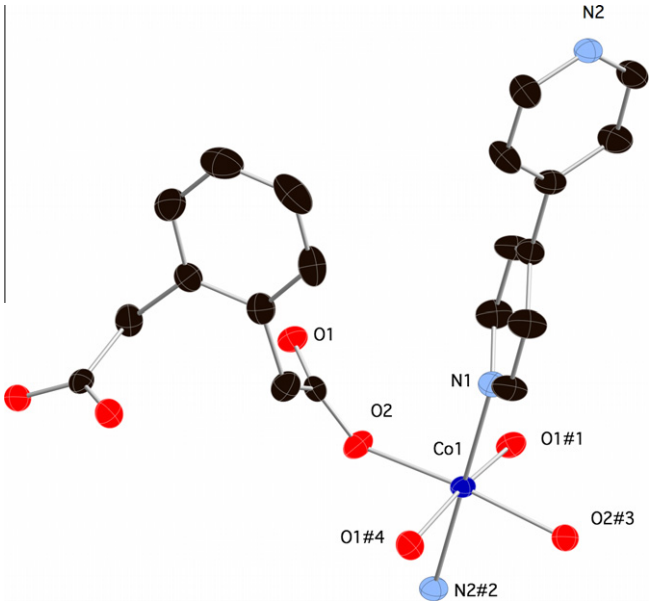

Fig. 5. Coordination environment of **3**. Symmetry codes refer to those in Table 5.

nitrogen donor atoms from three different bpy ligands in a meridional arrangement, *trans* oxygen atom donors from two ophda ligands, and an aqua ligand (Fig. 2b). Bond lengths and angles within the respective coordination environments are listed in Table 4.

Bis(monodentate) ophda ligands with a μ_2-κ^2-O:O′ binding mode (Scheme 2) link Co2 atoms into $[Co(ophda)(H_2O)]_n$ 1-D chains, which have Co···Co through-ligand contact distances of 9.725 Å. This longer through-ligand distance, when compared to that in **1**, is promoted by the wider torsion angle of 145.4° between the ophda acetate arms. These $[Co(ophda)(H_2O)]_n$ chains are linked into 2-D $[Co(ophda)(bpy)(H_2O)]_n$ (4,4) grid layer submotifs (Fig. 3a) by bpy ligands with an inter-ring torsion angle of 5.4°, which provide Co···Co contacts measuring 11.455 Å. Pairs of $[Co(ophda)(bpy)(H_2O)]_n$ layers are connected by crystallographically distinct bpy tethers with virtually flat conformation (inter-ring torsion = 0.5°) into neutral $[Co_2(ophda)_2(bpy)_3(H_2O)_2]_n$ coordination polymer slabs (Fig. 3b). These pillaring bpy molecules span a Co···Co contact distance of 11.379 Å. Treating the cobalt atoms within the slabs as 5-connected nodes produces a very uncommon bilayer network with $4^8 6^2$ SnS topology (Fig. 3c). Similar slab motifs with a 2:5 metal:tether ratio have been seen in the coordination polymers $[Cd(isonicotinate)_2(dpe)_{0.5}(H_2O)]_n$ [31] and $\{[Ag(pyz)_2][Ag_2(pyz)_5](PF_6)_3{\cdot}2CH_2Cl_2\}_n$ (pyz = pyrazine) [32]. The pillared bilayers in **2** can be considered as slices of a standard primitive cubic topology.

Incipient 1-D cuboid channels coursing through the bilayer slab motifs of **2** contain unligated bpy molecules, which occupy 24.7% of the unit cell volume according to PLATON [33]. These engage in hydrogen bonding acceptance from unligated water molecules in their vicinity (Table 3). The presence of the unligated bpy molecules appears to prevent the 2D + 2D → 3D interpenetration of bilayer motifs seen in the previously reported cadmium isonicotinate phase [31].

Situated between individual $[Co_2(ophda)_2(bpy)_3(H_2O)_2]_n$ coordination polymer slabs are the isolated $[Co(H_2O)_4(bpy)_2]^{2+}$ coordination complex cations, unligated nitrate ions required for charge balance, and numerous water molecules of crystallization (Fig. 4). The complex cations are anchored to the $[Co_2(ophda)_2(bpy)_3(H_2O)_2]_n$ slabs by hydrogen bonding donation from their aqua

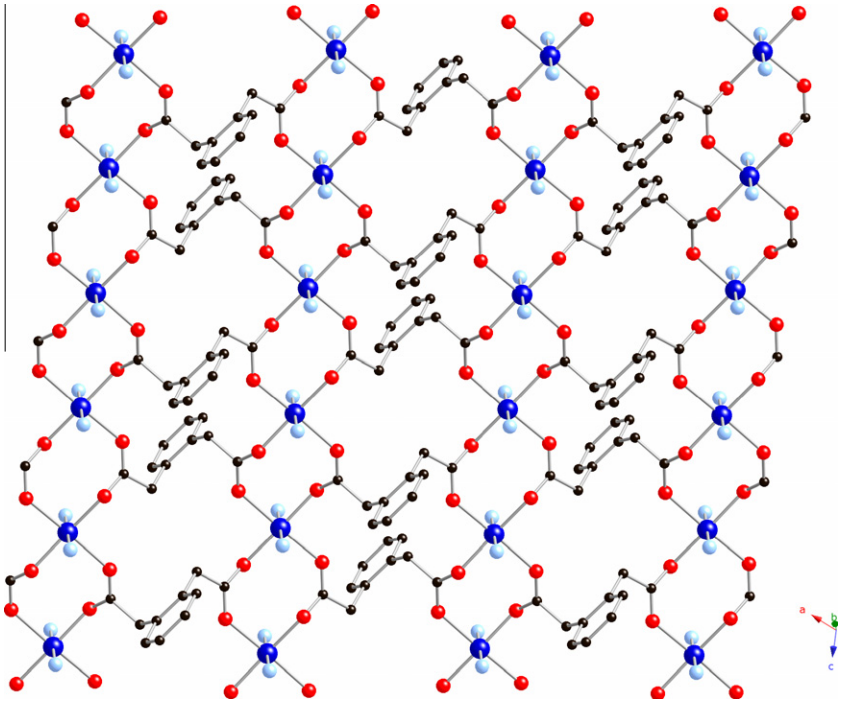

Fig. 6. $[Co(ophda)]_n$ layer in **3**.

ligands to unligated ophda carboxylate oxygen atoms. They also engage in hydrogen bonding to each other to form supramolecular ribbons, via their aqua ligands and pendant pyridine rings of their bpy ligands. Information regarding these hydrogen-bonding interactions is listed in Table 3. Co-crystallized charged coordination complexes are rarely seen in divalent metal carboxylate coordination polymers, although a divalent copper phase reported by Shimizu provides some precedent [34]. This material consists of $[Cu(dpe)(H_2O)_2]_n^{2n+}$ grids cationic encapsulating octahedrally coordinated $[Cu(4\text{-pyridinesulfonate})_4(H_2O)_2]^{2-}$ anions. To the best of our knowledge, cationic complexes of the generic type $[M(H_2O)_4L_2]^{2+}$ have never been entrained within a carboxylate coordination polymer framework.

3.4. Structural description of $[Co(ophda)(bpy)]_n$ (**3**)

The asymmetric unit of compound **3** consists of a divalent cobalt atom on a crystallographic 2-fold rotation axis, half of a bpy ligand whose central C–C σ bond and nitrogen atoms are situated along the same axis, and half of an ophda ligand bisected by another crystallographic 2-fold rotation axis. The coordination environment at cobalt is an axially compressed $\{CoN_2O_4\}$ octahedron (Fig. 5) with trans bpy pyridyl nitrogen donors in equatorial positions. Oxygen donor atoms from four different ophda ligands complete the coordination sphere, with two occupying trans equatorial positions and two taking up the shortened axial positions. Bond lengths and angles within the coordination environment are listed in Table 4.

Exotetradentate ophda ligands, with a μ_4-κ^4-O:O′:O″:O‴ binding mode (Scheme 2) and a torsion angle of 127.6° between their acetate arms, link the divalent cobalt atoms into 2-D $[Co(ophda)]_n$ coordination polymer layers (Fig. 6). Bridging of adjacent cobalt ions in *syn-anti* fashion by the pendant arm acetate groups of the ophda ligands produces 1-D $[Co(OCO)_2]_n$ chain submotifs containing *spiro*-fused {Co(OCO)Co(OCO)} 8-membered rings, whose Co···Co through-space contact distances measure 4.871 Å. The closest inter-chain Co···Co contact distances, through the full span of the ophda ligands, is 8.173 Å. If both the cobalt atoms and ophda ligands are considered connecting nodes, the $[Co(ophda)]_n$ grid patterns can be construed as simple 4-connected regular (4,4) nets.

Parallel $[Co(ophda)]_n$ layers are pillared into a non-interpenetrated $[Co(ophda)(bpy)]_n$ 3-D coordination polymer network by tethering bpy ligands (Fig. 7a), which span a Co···Co contact distance of 11.434 Å. The inter-ring torsion angle within the bpy ligands is 62.0°. Thus, the cobalt atoms in **3** can be construed as 6-connected nodes, joining to four 4-connected ophda ligand nodes within a single $[Co(ophda)]_n$ layer, and to cobalt atoms in two adjacent $[Co(ophda)]_n$ layers via bpy tethers. Topological analysis with TOPOS software [35] reveals an underlying non-interpenetrated 4,6-connected binodal **fsc** net (Fig. 7b) with a Schläfli symbol of $(4^46^2)(4^46^{10}8)$ and a long Vertex Symbol of $[4.4.4.4.6_2.6_2][4.4.4.4.6_5.6_5.6_5.6_5.6_5.6_5.6_5.*.*.*]$. This net can be considered a derivative of the commonly encountered 6-connected primitive cubic **pcu** net, but with two *trans* pillars removed at every other node. This **fsc** net is seldom encountered in coordination polymer chemistry, with the cluster-based species $[(CuI)_7(DABCO)_{2.5}]_n$ [36] and pillared sheet coordination polymer $[Cd(\mu_4\text{-}SO_4)(bpy)]_n$ [37] being among the few reported examples.

3.5. Magnetic properties of **3**

A variable temperature magnetic susceptibility study was carried out on a polycrystalline sample of **3** to probe magnetic superexchange between the $S = 3/2$ Co^{2+} ions within the 1-D $\{Co(OCO)_2\}_n$ chain motifs. For magnetic behavior in divalent cobalt complexes with tetragonally distorted octahedral coordination environments, both magnetic superexchange (J) and single ion effects such as zero-field splitting (D) must be taken into account. A phenomenological expression by Rueff (Eq. (1)) can estimate the cooperative effect of these parameters, and has been successfully applied in the modeling of the magnetic behavior of $S = 3/2$ chains [38].

$$\chi_m^T = A\exp(-D/kT) + B\exp(J/kT) \quad (1)$$

where $A + B = C = (5Ng^2\beta^2/4k)$.

The $\chi_mT(T)$ data for **3** were fit to Eq. (1), with the best fit values $A = 0.81(6)$ cm^3 K mol^{-1} and $B = 2.42(3)$ cm^3 K mol^{-1} (giving

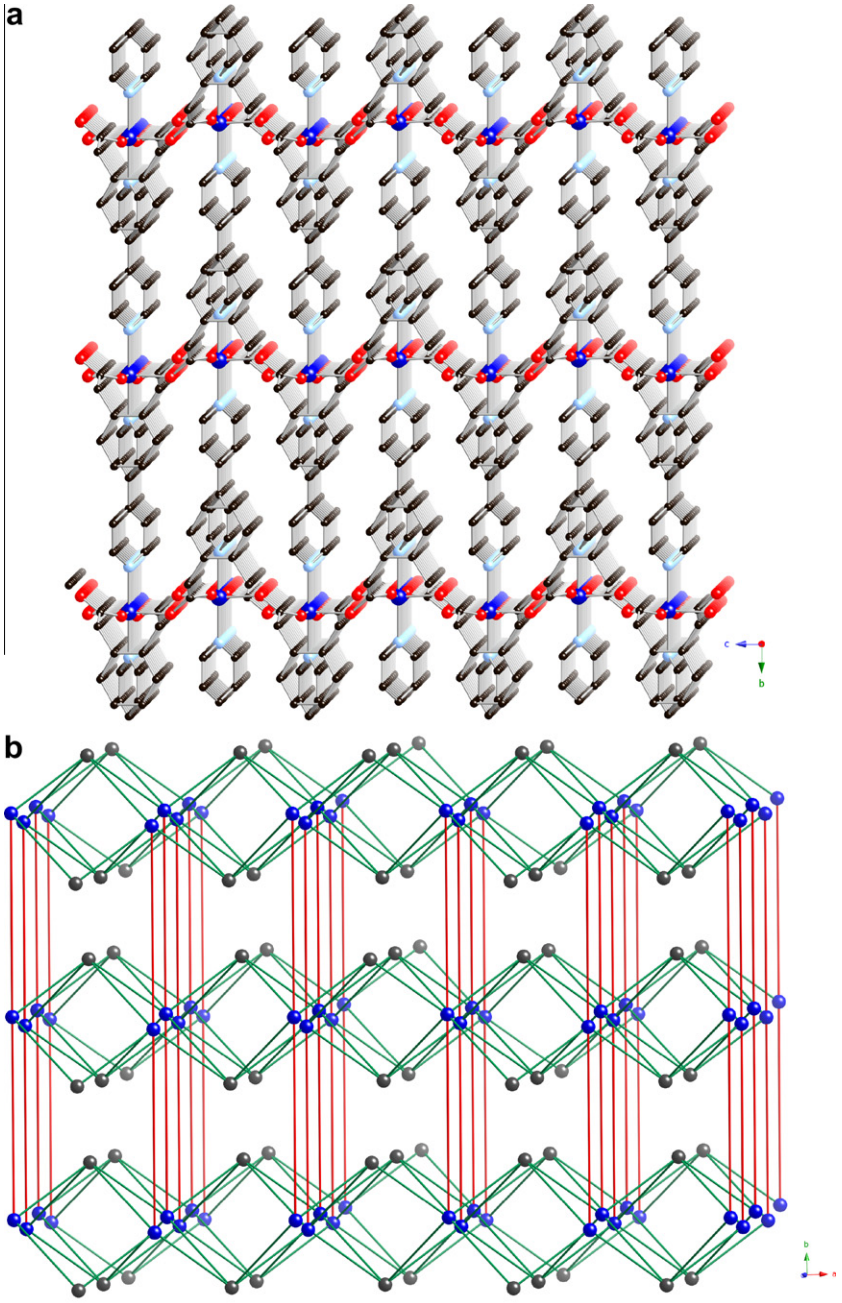

Fig. 7. (a) $[Co(ophda)(bpy)]_n$ 3-D network (b) schematic perspective of 4,6-binodal $(4^46^2)(4^46^{10}8)$ **fsc** topology in **3**. In the web version of this article, 6-connected cobalt nodes and 4-connected ophda nodes are shown in blue and gray, respectively, while pillaring bpy ligands are represented as red sticks. (For interpretation of the references to colour in this figure legend, the reader is referred to the web version of this article.)

$g = 2.23$), $J = +1.5(2)\ cm^{-1}$ and $D = 30(1)\ cm^{-1}$, with $R = 1.0 \times 10^{-3} = \{\Sigma[(\chi_mT)_{obs} - (\chi_mT)_{calc}]^2/\Sigma[(\chi_mT)_{obs}]^2\}$ (Fig. 8). The positive J indicates the presence of ferromagnetic superexchange along the $\{Co(OCO)_2\}_n$ chains in **3**, revealed by the large upsurge in χ_mT value below 20 K. However this ferromagnetism acts cooperatively with single ion effects, which serves to reduce the $\chi_mT(T)$ product value as temperature decreases from 300 K to 20 K. It should be noted that the fit to Eq. (1) is somewhat mediocre, so the best-fit values should be taken as only estimates. No field-dependent hysteresis was observed at 2 K.

3.6. Thermogravimetric analysis

Polycrystalline samples of compounds **1–3** were subjected to thermogravimetric analysis under flowing N_2 in order to probe their thermal stability. Compound **1** lost 4.5% of its mass between 85 °C and 150 °C, consistent with loss of its aqua ligands (4.0% calc'd). The mass remained stable until 300 °C, at which temperature the organic components were pyrolyzed. The final mass remnant of 19.3% at 475 °C is consistent with a deposition of CoO (16.6% calc'd) along with some carbonaceous material. For compound **2**, an initial mass loss of 6.3% between 25 and 75 °C matches exactly with the loss of all unligated water molecules. A subsequent 27.8% mass loss between 75 and 230 °C corresponds to the ejection of the free bpy molecules, ligated water molecules, and nitrate ions (27.1% calc'd combined). The final mass remnant of 13.7% at 475 °C is likely CoO (11.2% calc'd) with some carbon-containing material. The mass of compound **3** remained stable until ~230 °C, when ligand ejection commenced. Degradation appeared to occur in two steps, one between ~230 and 275 °C and the other between

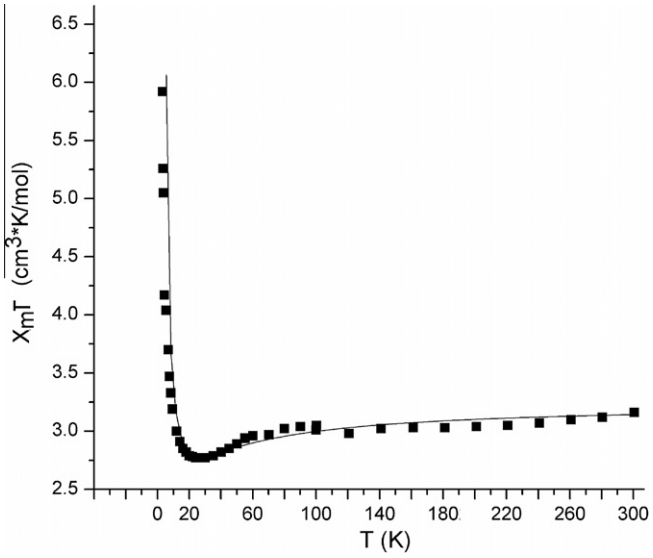

Fig. 8. A plot of $\chi_m T$ vs T for **3**. The thin line indicates the best fit to Eq. (1).

~310 and 330 °C. The final mass remnant of 26.1% at 475 °C likely represents a mixture of $CoCO_3$ (29.2% calc'd) and CoO (18.4% calc'd). Thermograms for **1**–**3** are shown in Figs. S2–S4.

4. Conclusions

The sparse structural chemistry of cobalt phenylenediacetate coordination polymers has been expanded with this study. The structure of **1** shows that extension of the *ortho* carboxylate arms does not appreciably alter coordination polymer dimensionality from that seen in its previously reported phthalate analog $[Co(pht)(dpe)(H_2O)]_n$. However, the longer arms of the ophda ligands appears to promote a monodentate/chelating binding mode, preventing "wrap around" 1,2-chelation and the exotridentate binding mode observed in the phthalate species. As a result the (4,4) grid topology of **1** is based on isolated cobalt atom nodes instead of *anti–syn* bridged dinuclear $\{Co_2(OCO)_2\}$ units. More notably, the anion-dependent topologies of the cobalt ophda/bpy coordination polymers **2** and **3** are not only both very rare, but differ tremendously from those seen in previous cobalt phthalate/bpy systems. In **2**, the exobidentate binding mode of the ophda ligands and the presence of coordination complex cations and small oxoanions appears to stabilize the uncommon 5-connected bilayer structure. In **3**, the ophda ligands bind in an exotetradentate fashion, allowing them to act as 4-connected nodes in the rarely seen 4,6-connected binodal **fsc** lattice. Additionally, the pendant carboxylate arms of the ophda ligands in **3** construct $\{Co(OCO)_2\}_n$ chain submotifs in which neighboring cobalt ions appear to undergo ferromagnetic superexchange. In this system, cooperative effects between acetate arm conformation and binding modes, along with the length of the dipodal nitrogen tether and the presence of co-crystallized charged species, act to instill the final coordination polymer topology during self-assembly.

Acknowledgments

Funding for this work was provided by the donors of the American Chemical Society Petroleum Research Fund. K.M.B. thanks the American Chemical Society SUMR program for her participation in the research. We thank Dr. Rui Huang for performing the elemental analyses, Ms. Amy Pochodylo for acquiring the magnetic data, and Mr. Chaun Gandolfo for spectral analysis.

Appendix A. Supplementary material

CCDC 806640, 806639, and 806638 contain the supplementary crystallographic data for complexes **1**, 2, and **3**, respectively. These data can be obtained free of charge from The Cambridge Crystallographic Data Centre via www.ccdc.cam.ac.uk/data_request/cif. Supplementary data associated with this article can be found, in the online version, at doi:10.1016/j.ica.2011.04.029.

References

[1] C. Janiak, Dalton Trans. (2003) 2781 (and references therein);
U. Mueller, M. Schubert, F. Teich, H. Puetter, K. Schierle-Arndt, J. Pastré, J. Mater. Chem. 16 (2006) 626.
[2] (a) L. Pan, D.H. Olson, L.R. Ciemnolonski, R. Heddy, J. Li, Angew. Chem., Int. Ed. 45 (2006) 616;
(b) M. Dinca, A.F. Yu, J.R. Long, J. Am. Chem. Soc. 128 (2006) 8904;
(c) J.L.C. Roswell, O.M. Yaghi, Angew. Chem., Int. Ed. 44 (2005) 4670;
(d) R. Matsuda, R. Kitaura, S. Kitagawa, Y. Kubota, R.V. Belosludov, T.C. Kobayashi, H. Sakamoto, T. Chiba, M. Takata, Y. Kawazoe, Y. Mita, Nature 436 (2005) 238;
(e) A.C. Sudik, A.R. Millward, N.W. Ockwig, A.P. Côté, J. Kim, O.M. Yaghi, J. Am. Chem. Soc. 127 (2005) 7110;
(f) X. Zhao, B. Xiao, A.J. Fletcher, K.M. Thomas, D. Bradshaw, M.J. Rosseinsky, Science 306 (2004) 1012;
(g) G. Férey, M. Latroche, C. Serre, F. Millange, T. Loiseau, A. Percheron-Guegan, Chem. Commun. (2003) 2976;
(h) H. Li, M. Eddaoudi, M. O'Keeffe, O.M. Yaghi, Nature 402 (1999) 276.
[3] (a) J.-R. Li, R.J. Kuppler, H.-C. Zhou, Chem. Soc. Rev. 38 (2009) 1477 (and references therein);
(b) A. Cingolani, S. Galli, N. Masciocchi, L. Pandolfo, C. Pettinari, A. Sironi, Chem. Eur. J. 14 (2008) 9890;
(c) J.S. Seo, D. Whang, H. Lee, S.I. Jun, J. Oh, Y.J. Jeon, K. Kim, Nature 404 (2000) 982.
[4] (a) Q.-R. Fang, G.-S. Zhu, M. Xue, J.-Y. Sun, S.-L. Qiu, Dalton Trans. (2006) 2399;
(b) X.-M. Zhang, M.-L. Tong, H.K. Lee, X.-M. Chen, J. Solid State Chem. 160 (2001) 118;
(c) O.M. Yaghi, H. Li, T.L. Groy, Inorg. Chem. 36 (1997) 4292.
[5] (a) J.Y. Lee, O.K. Farha, J. Roberts, K.A. Scheidt, S.T. Nguyen, J.T. Hupp, Chem. Soc. Rev. 38 (2009) 1450 (and references therein);
(b) L. Ma, C. Abney, W. Lin, Chem. Soc. Rev. 38 (2009) 1248 (and references therein);
(c) S.G. Baca, M.T. Reetz, R. Goddard, I.G. Filippova, Y.A. Simonov, M. Gdaniec, N. Gerbeleu, Polyhedron 25 (2006) 1215;
(d) H. Han, S. Zhang, H. Hou, Y. Fan, Y. Zhu, Eur. J. Inorg. Chem. 8 (2006) 1594;
(e) C.-D. Wu, A. Hu, L. Zhang, W. Lin, J. Am. Chem. Soc. 127 (2005) 8940;
(f) W. Mori, S. Takamizawa, C.N. Kato, T. Ohmura, T. Sato, Microporous Mesoporous Mater. 73 (2004) 31;
(g) N. Guillou, Q. Gao, P.M. Forster, J.S. Chang, M. Noguès, S.-E. Park, G. Férey, A.K. Cheetham, Angew. Chem., Int. Ed. 40 (2001) 2831.
[6] (a) M.D. Allendorf, C.A. Bauer, R.K. Bhakta, R.J.T. Houk, Chem. Soc. Rev. 38 (2009) 1330 (and references therein);
(b) J. He, J. Yu, Y. Zhang, Q. Pan, R. Xu, Inorg. Chem. 44 (2005) 9279;
(c) S. Wang, Y. Hou, E. Wang, Y. Li, L. Xu, J. Peng, S. Liu, C. Hu, New J. Chem. 27 (2003) 1144;
(d) L.G. Beauvais, M.P. Shores, J.R. Long, J. Am. Chem. Soc. 122 (2000) 2763.
[7] (a) S. Zang, Y. Su, Y. Li, Z. Ni, Q. Meng, Inorg. Chem. 45 (2006) 174;
(b) L. Wang, M. Yang, G. Li, Z. Shi, S. Feng, Inorg. Chem. 45 (2006) 2474.
[8] D.J. Tranchemontagne, J.L. Mendoza-Cortés, M. O'Keeffe, O.M. Yaghi, Chem. Soc. Rev. 38 (2009) 1257 (and references therein).
[9] M. Kurmoo, Chem. Soc. Rev. 38 (2009) 1353 (and references therein).
[10] S. Xiang, X. Wu, J. Zhang, R. Fu, S. Hu, X. Zhang, J. Am. Chem. Soc. 127 (2005) 16352.
[11] X.-Y. Wang, S.C. Sevov, Inorg. Chem. 47 (2008) 1037.
[12] Y.-G. Huang, D.-Q. Yuan, L. Pan, F.-L. Jiang, M.-Y. Wu, X.-D. Zhang, W. Wei, Q. Gao, J.Y. Lee, J. Li, M.-C. Hong, Inorg. Chem. 46 (2007) 9609.
[13] P. Lightfoot, A. Snedden, J. Chem. Soc., Dalton Trans. (1999) 3549.
[14] C.Y. Sun, L.C. Li, L.P. Jin, Polyhedron 25 (2006) 3017.
[15] S.W. Lee, H.J. Kim, Y.K. Lee, K. Park, J. Son, Y. Kwon, Inorg. Chim. Acta 353 (2003) 151.
[16] M.A. Braverman, R.M. Supkowski, R.L. LaDuca, Inorg. Chim. Acta 360 (2007) 2353.
[17] X.-N. Cheng, W.-X. Zhang, Y.-Y. Lin, Y.-Z. Zheng, X.-M. Chen, Adv. Mater. 19 (2007) 1494.
[18] J. Tao, M. Tong, X. Chen, J. Chem. Soc., Dalton Trans. (2000) 3669.
[19] F. Yang, Y. Ren, D. Li, F. Fu, G. Qi, Y. Wang, J. Mol. Struct. 892 (2008) 283.
[20] X. Xie, S. Chen, Z. Xia, S. Gao, Polyhedron 28 (2009) 679.
[21] Z. Chen, Q. Zhao, W. Xiong, Z. Zhang, F. Liang, Z. Anorg. Allg. Chem. 636 (2010) 2691.
[22] K.M. Blake, M.A. Braverman, J.H. Nettleman, L.K. Sposato, R.L. LaDuca, Inorg. Chim. Acta 363 (2010) 3966.
[23] M.A. Braverman, R.L. LaDuca, Cryst. Growth Des. 7 (2007) 2343.

[24] K.M. Blake, L.L. Johnston, J.H. Nettleman, R.M. Supkowski, R.L. LaDuca, CrystEngComm 12 (2010) 1927.
[25] F.H. Allen, Acta Crystallogr., Sect. B 58 (2002) 380.
[26] O. Kahn, Molecular Magnetism, VCH Publishers, New York, 1993.
[27] SAINT, Software for Data Extraction and Reduction, Version 6.02 Bruker AXS, Inc., Madison, WI, 2002.
[28] SADABS, Software for Empirical Absorption Correction, Version 2.03 Bruker AXS, Inc., Madison, WI, 2002.
[29] G.M. Sheldrick, SHELXTL, Program for Crystal Structure Refinement, University of Göttingen, Göttingen, Germany, 1997.
[30] M. Kurmoo, C. Estournes, Y. Oka, H. Kumagai, K. Inoue, Inorg. Chem. 44 (2005) 217.
[31] Z. Fu, X. Wu, J. Dai, L. Wu, C. Cui, S. Hu, Chem. Commun. (2001) 1856.
[32] L. Carlucci, G. Ciani, D.M. Proserpio, A. Sironi, Angew. Chem., Int. Ed. 31 (1995) 1895.
[33] A.L. Spek, PLATON, A Multipurpose Crystallographic Tool, Utrecht University, Utrecht, The Netherlands, 1998.
[34] L.J. May, G.K.H. Shimizu, Chem. Commun. (2005) 1270.
[35] V.A. Blatov, A.P. Shevchenko, V.N. Serezhkin, J. Appl. Crystallogr. 33 (2000) 1193.
[36] M. Bi, G. Li, J. Hua, Y. Liu, X. Liu, Y. Hu, Z. Shi, Cryst. Growth Des. 7 (2007) 2066.
[37] Y. Xu, W. Bi, X. Li, D. Sun, R. Cao, M. Hong, Inorg. Chem. Commun. 6 (2003) 495.
[38] J.M. Rueff, N. Masciocchi, P. Rabu, A. Sironi, A. Skoulios, Eur. J. Inorg. Chem. (2001) 2843.